Since January 2020 Elsevier has created a COVID-19 resource centre with free information in English and Mandarin on the novel coronavirus COVID-19. The COVID-19 resource centre is hosted on Elsevier Connect, the company's public news and information website.

Journal Pre-proof

Modified susceptible-exposed-infectious-recovered model for assessing the effectiveness of non-pharmaceutical interventions during the COVID-19 pandemic in Seoul

Seungpil Jung, Jong-Hoon Kim, Seung-Sik Hwang, Junyoung Choi, Woojoo Lee

PII: S0022-5193(22)00320-4
DOI: https://doi.org/10.1016/j.jtbi.2022.111329
Reference: YJTBI 111329

To appear in: *Journal of Theoretical Biology*

Received date : 16 June 2022
Revised date : 6 October 2022
Accepted date : 13 October 2022

Please cite this article as: S. Jung, J.-H. Kim, S.-S. Hwang et al., Modified susceptible-exposed-infectious-recovered model for assessing the effectiveness of non-pharmaceutical interventions during the COVID-19 pandemic in Seoul. *Journal of Theoretical Biology* (2022), doi: https://doi.org/10.1016/j.jtbi.2022.111329.

Modified susceptible-exposed-infectious-recovered model for assessing the effectiveness of non-pharmaceutical interventions during the COVID-19 pandemic in Seoul

Seungpil Jung[a], Jong-Hoon Kim[b], Seung-Sik Hwang[a], Junyoung Choi[c] and Woojoo Lee[a,*]

[a]*Department of Public Health Sciences, Graduate School of Public Health, Seoul National University, 1 Gwanak-ro, Gwanak-gu, Seoul, 08826, Republic of Korea*

[b]*International Vaccine Institute, SNU Research Park, 1 Gwanak-ro, Gwanak-gu, Seoul, 151-742, Republic of Korea*

[c]*Center for Data Science, Seoul Institute of Technology, 37 Maebongsan-ro, Mapo-gu, Seoul, 03909, Republic of Korea*

ARTICLE INFO

Keywords:
SARS-CoV-2
COVID-19
SEIR model
Social distancing
Ban on gatherings
Mobility

ABSTRACT

Susceptible-exposed-infectious-recovered (SEIR) models were applied to assess the effectiveness of non-pharmaceutical interventions (NPIs) and to study the dynamic behavior of the COVID-19 pandemic. Recently, SEIR models have evolved to address the change of human mobility by some NPIs for predicting the new confirmed cases. However, the models have serious limitations when applied to Seoul. Seoul has two representative quarantine policies, i.e. social distancing and the ban on gatherings. Effects of the two policies need to be reflected in different functional forms in the model because changes in human mobility do not fully reflect the ban on gatherings. Thus we propose a modified SEIR model to assess the effectiveness of social distancing, ban on gatherings and vaccination strategies. The application of the modified SEIR model was illustrated by comparing the model output with real data.

1. Introduction

The first case of severe acute respiratory syndrome coronavirus 2 (SARS-CoV-2) was documented in early December 2019 in Wuhan, China, and by the end of November 2021, more than 260 million cases of coronavirus disease (COVID-19) had been reported (World Health Organization [WHO], 2021). To prevent the spread of COVID-19, many countries have adopted non-pharmaceutical interventions (NPIs) such as travel restrictions and social distancing. Countries have also initiated COVID-19 vaccination to achieve herd immunity. For example, the United States approved Pfizer-BioNTech and Moderna vaccines for emergency use authorization near the end of 2020 (Food and Drug Administration [FDA], 2022).

In Seoul, the capital of South Korea, more than 450,000 confirmed cases and 3,500 deaths have been reported by the end of November 2021, since the first case was detected on January 24, 2020, (Ministry of Health and Welfare [MOHW], 2022). To prevent transmission, a social distancing policy was implemented in Korea on March 22, 2020, which was tightened and relaxed depending on the pandemic situation (MOHW, 2020). The social distancing rule in Korea includes reducing group events, face-to-face reporting, self-isolation of mild COVID-19 patients, and isolation of severe COVID-19 patients. In addition, the ban on gatherings, which restricts the number of people gathered in commercial facilities, was introduced on December 23, 2020. Vaccination for COVID-19 was initiated in February 2021. The rate of full vaccination (one dose of Janssens or two doses of Pfizer-BioNTech, Moderna, or AstraZeneca) in Seoul was 76.7% at the end of October 2021. Despite this high vaccination coverage, the daily number of new confirmed cases was more than 1000 after November 2021, and the preventive effect of vaccines against variants of the virus appears to be lower than that against the original strain (Lopez Bernal et al., 2021). Implementing NPIs is important, even after vaccine introduction. Thus the effectiveness of different NPIs should be examined in various pandemic situations.

Mathematical models for the COVID-19 pandemic have been proposed to assess the effectiveness of NPIs and study the dynamic behavior of the pandemic (Medeiros-Sousa et al., 2021; Zhou et al., 2020; Wu et al., 2020; Britton et al., 2020; Chang et al., 2021). Recently reported models have utilized human mobility to predict the number of new

*Corresponding author.
E-mail address: lwj221@gmail.com (W. Lee)

confirmed cases under various NPI scenarios. Zhou et al. (2020) and Wu et al. (2020) used a susceptible-exposed-infectious-recovered (SEIR) model with mobile-based sighting data and the daily number of passengers using public transportation, respectively, to determine the effect of human mobility restrictions. Chang et al. (2021) extended the SEIR model to decompose the transmission of COVID-19 into residence-induced and facility-induced cases using SafeGraph mobility data (SafeGraph, 2020).

However, these models have serious limitations when applied to megacities such as Seoul. First, the two representative quarantine policies—social distancing and bans on gatherings—must be reflected in different functional forms in the mathematical model. For example, without considering different functional forms, the reduction in the daily number of new confirmed cases in Seoul after the ban on gatherings (December 23, 2020) can be explained only by approximately 58% reduction in mobility, which is unrealistic in practical scenarios. Thus, the ban on gatherings should be expressed in a different functional form in a mathematical model. Second, Chang et al. (2021)'s extended SEIR model requires accurate information about the location of an individual, which is difficult to obtain in Seoul because the facilities and residential areas are intermixed.

Considering these points, we have developed a modified SEIR model to address the effectiveness of social distancing, bans on gatherings, and vaccination. Based on this model, we assess the effects of NPIs under various hypothetical scenarios. The usefulness of the proposed SEIR model is illustrated by comparing the model outputs with real data.

2. Data

Seoul, the capital of Korea, is home to nearly ten million people. The city has 25 districts (called "gu") and 426 wards (called "dong").

2.1. Epidemiological data

The Seoul Open Data Plaza, formally operated by the city of Seoul, shares public data on various topics. We collected the daily number of new confirmed cases, fully vaccinated cases, and population in each gu. The daily number of new confirmed cases is available at https://data.seoul.go.kr/dataList/OA-20470/S/1/datasetView.do. MOHW (2020) defines a confirmed case as a person who tested positive for the infectious SARS-CoV-2 pathogen by using reverse transcription-polymerase chain reaction (RT-PCR), regardless of the clinical manifestations. Figure 1 shows the moving average of the daily number of new confirmed cases in Seoul from November 2020 to November 2021, with the history of various interventions indicated by colored vertical lines. This trend decreased sharply when the ban on gatherings (purple dashed line) was implemented with social distancing, and the number of new confirmed cases increased rapidly when social distancing was relaxed in November 2021.

After the vaccine was developed in 2021, vaccinations for healthcare workers and people aged $\geq$ 75 years began in South Korea. The first vaccination in Seoul was administered on the last day of February, as represented by the green dotted line in Figure 1. The daily number of vaccinated individuals in Seoul was also provided by the Seoul Open Data Plaza, which is available at http://data.seoul.go.kr/dataList/OA-20914/S/1/datasetView.do. The number of resident registration populations in each gu is available at https://data.seoul.go.kr/dataList/419/S/2/datasetView.do.

2.2. Human mobility data

Oliver et al. (2020) emphasized human mobility data are important for investigating the transmission of COVID-19 and for evaluating NPIs. We explored the value of mobile phone data using detailed call records in COVID-19 research. Badr et al. (2020) studied the association between COVID-19 transmission and mobility patterns, which is in the form of origin-destination (OD) matrices, in the USA. Nouvellet et al. (2021) analyzed the association between mobility patterns, sourced from Apple or Android devices, and transmission rates of COVID-19 under varying control measures. Considering these points, we collaborated with SK telecom, South Korea's largest mobile service provider, and developed an algorithm to produce OD matrices by using call detail records. The algorithm for constructing OD matrices consists of the following three steps: The first step is recording the locations (in our application, dong) where each mobile user remained for more than 30 min every hour. The second step is generating structured data representing the order of the locations and durations for which each mobile user stayed, and the third step is to transform the structured data for the individual mobility information into an OD matrix.

Figure 2 illustrates the workflow of this algorithm. In Figure 2a, a person with ID = 1 begins to move at 10:47, travels through B, arrives at C at 11:15, and remains at this location for 42 min. In this case, this person is recorded

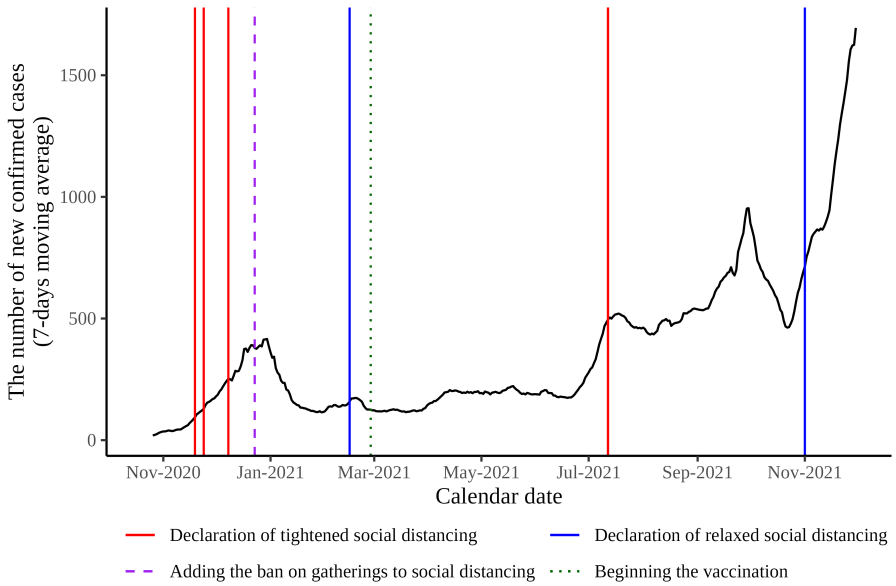

Figure 1: Number of COVID-19 confirmed cases and history of NPIs in Seoul

as having two stays at A and C because more than 30 min were spent in these locations. Following the same logic, a person with ID = 2 recorded two movements from A to B and B to A, as shown in Figure 2a. The mobility information is then transformed into an OD matrix. The movement of ID=1 from A to C adds 1 to the corresponding cell of the OD matrix, and the movements of ID=2 from A to B and B to A also add 1 to each cell corresponding to the movements. Therefore, one person was allowed to contribute to the counts in the OD matrix several times.

SK telecom provided an OD matrix for each day from March 2021 to June 2021, which limited the research period. To overcome this limitation, we employed other mobility data provided by the Transport Operation and Information Service (TOPIS). The TOPIS mobility data summarize the transportation card usage data from Korea Smart Card Co., Ltd. (Seoul, Korea) and are available at https://topis.seoul.go.kr/refRoom/openRefRoom_3_4.do. TOPIS mobility describes the number of passengers on public transportation using the trip-chain method (Kim, 2007), which does not count transfers but counts the movement between two dongs.

2.3. Commercial facility data

Lim et al. (2022) showed that 55.7% of confirmed cases were caused by mass infection, which occurred in various facilities such as restaurants, sports facilities, and entertainment businesses. To prevent mass infection, the Korean government has prohibited private gatherings of more than five people in most places, including restaurants and party rooms, on December 23, 2020. This policy presumes that the transmission of COVID-19 strongly depends on the number of commercial facilities, and was reflected in our new SEIR model. We determined the number of commercial facilities by gu using the Trade Area Analysis Service. These facilities include various shops (bakery, coffee shops, bar, fast-food, etc.), the service industries (institute, hospital, etc.), and retail businesses (supermarkets, convenience stores, etc.). Figure 3 shows the regional distribution of the commercial facilities in Seoul. In Gangnam-gu, which is the central business district, the number of commercial facilities is much higher than that in other regions. By contrast, Geumcheon-gu, a residential city, has a relatively small number of commercial facilities. These data are available at https://golmok.seoul.go.kr/regionAreaAnalysis.do.

3. Methods

To assess the effectiveness of the NPIs, we employed the SEIR model, which conveniently reveals the relationship between physical and model parameters. Choi and Ki (2020) and Kondo (2021) used the SEIR model for similar

(a)

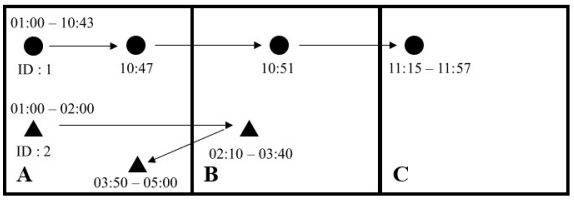

(b)

ID	Date	Hour	Location
1	2020-01-01	1	A
⋮	⋮	⋮	⋮
1	⋮	10	A
1	⋮	11	C
2	⋮	1	A
2	⋮	2	B
2	⋮	3	B
2	2020-01-01	4	A

(c)

Origin \ Destination	A	B	C
A	0	1	1
B	1	0	0
C	0	0	0

Figure 2: Algorithm for producing the OD matrix. (a) Physical path for each mobile user in dong AC. (b) Structured data consisting of time and path information. (c) OD matrix.

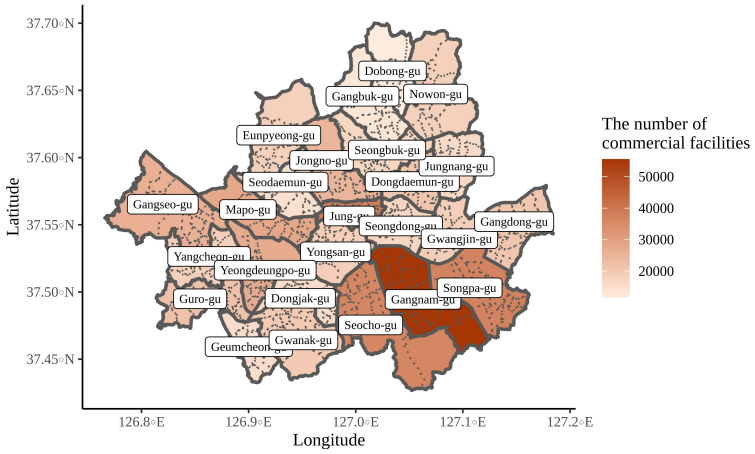

Figure 3: Regional distribution of commercial facilities in Seoul.

reasons. In this section, we review the traditional SEIR model and an extended version incorporating mobility information by Chang et al. (2021), and explains the new modified SEIR model for the COVID-19 situation in Seoul.

3.1. Traditional SEIR models

Suppose that $S^{(t)}$, $E^{(t)}$, $I^{(t)}$, and $R^{(t)}$ denote the number of susceptible, exposed, infected, and recovered individuals at time t, respectively. The deterministic SEIR model can be represented by a set of ordinary differential

equations:

$$\frac{dS^{(t)}}{dt} = -\beta\frac{S^{(t)}I^{(t)}}{N} \qquad \frac{dE^{(t)}}{dt} = \beta\frac{S^{(t)}I^{(t)}}{N} - \frac{1}{\delta_E}E^{(t)}$$
$$\frac{dI^{(t)}}{dt} = \frac{1}{\delta_E}E^{(t)} - \frac{1}{\delta_I}I^{(t)} \qquad \frac{dR^{(t)}}{dt} = \frac{1}{\delta_I}I^{(t)}$$
$$N = S^{(t)} + E^{(t)} + I^{(t)} + R^{(t)}$$

where β is the transmission rate; N is the total population size; and δ_E and δ_I represent the latent and infectious periods, respectively. $\frac{dS^{(t)}}{dt}$ describes how a susceptible group moves into an exposed group and is proportional to the transmission rate and the current number of infected people. $\frac{dE^{(t)}}{dt}$ is the sum of the two values. The first value represents the new exposed individuals from the susceptible group and second value represents the number of individuals who progress to the infected group. The other parts of the equation can be interpreted in a similar manner. The deterministic model is mechanistically interpretable and easy to implement. This approach is less natural than stochastic models, because the spread of infectious diseases is close to stochastic. In addition, a stochastic model is required to systematically assess uncertainty in parameter estimates (Andersson and Brittion, 2000).

Stochastic variants of the SEIR model have been developed to overcome the limitations of deterministic models (Becker, 1981; Abbey, 1952; Lekone and Finkenstadt, 2006). For example, Lekone and Finkenstadt (2006) developed the following discrete-time stochastic SEIR model:

$$S^{(t+1)} = S^{(t)} - N^{(t)}_{S\to E} \qquad E^{(t+1)} = E^{(t)} + N^{(t)}_{S\to E} - N^{(t)}_{E\to I}$$
$$I^{(t+1)} = I^{(t)} + N^{(t)}_{E\to I} - N^{(t)}_{I\to R} \qquad R^{(t+1)} = R^{(t)} + N^{(t)}_{I\to R}$$
$$N^{(t)}_{S\to E} \sim \text{Binomial}\left(S^{(t)}, 1 - e^{-\beta(t)I^{(t)}/N}\right) \qquad N^{(t)}_{E\to I} \sim \text{Binomial}\left(E^{(t)}, 1 - e^{-1/\delta_E}\right)$$
$$N^{(t)}_{I\to R} \sim \text{Binomial}\left(I^{(t)}, 1 - e^{-1/\delta_I}\right) \qquad N = S^{(t)} + E^{(t)} + I^{(t)} + R^{(t)}$$

where $N^{(t)}_{S\to E}$, $N^{(t)}_{E\to I}$ and $N^{(t)}_{I\to R}$ are the numbers of individuals who transition between compartments represented by binomial random variables. $\beta(t)$ is the time-dependent transmission rate and δ_E and δ_I represent the latent and infectious periods, respectively. The stochastic SEIR model allows computation of the prediction interval based on Monte Carlo simulations (Xie, 2020).

Considering that social distancing and bans on gatherings are typical examples of NPIs that substantially affect human mobility and transmission patterns, traditional SEIR models are not suitable for evaluating the impact of NPIs because they do not explicitly consider human mobility. Therefore, we review a recent extended SEIR model to incorporate human mobility information in a systematic manner (Chang et al., 2021).

3.2. An extended SEIR (ESEIR) model using mobility information

Chang et al. (2021) developed an extension of the stochastic SEIR model using SafeGraph mobility data. SafeGraph defines census block groups (CBGs) and points of interest (POIs) as geographical units used by the United States Census Bureau and specific locations that a person may visit. It records the number of people moving from CBGs to POIs (SafeGraph, 2020).

Let $c_i (i = 1, ..., m)$ and $p_j (j = 1, ..., n)$ denote the ith CBG and jth POI, respectively. Then, Chang et al. (2021)'s ESEIR model can be described as

$$N^{(t)}_{S_{c_i}\to E_{c_i}} \sim \text{Poisson}\left(\frac{S^{(t)}_{c_i}}{N_{c_i}}\sum_{j=1}^{n}\lambda^{(t)}_{p_j}w^{(t)}_{ij}\right) + \text{Binomial}\left(S^{(t)}_{c_i}, \lambda^{(t)}_{c_i}\right) \tag{1}$$

$$N^{(t)}_{E_{c_i}\to I_{c_i}} \sim \text{Binomial}\left(E^{(t)}_{c_i}, \frac{1}{\delta_E}\right), \qquad N^{(t)}_{I_{c_i}\to R_{c_i}} \sim \text{Binomial}\left(I^{(t)}_{c_i}, \frac{1}{\delta_I}\right) \tag{2}$$

where $w_{ij}^{(t)}$ represents the number of visitors from c_i to p_j, $\lambda_{c_i}^{(t)}$ and $\lambda_{p_j}^{(t)}$ represent the infection rates at c_i and p_j at time t, respectively. The infection rates at the POIs and CBGs are expressed as

$$\lambda_{p_j}^{(t)} = \psi d_{p_j}^2 \frac{I_{p_j}^{(t)}}{a_{p_j}}, \qquad \lambda_{c_i}^{(t)} = \beta_{\text{base}} \frac{I_{c_i}^{(t)}}{N_{c_i}}$$

where d_{p_j} is the dwell time fraction of visitors at p_j, a_{p_j} is the physical area of p_j, $I_{p_j}^{(t)}$ is the number of infected people at p_j, and β_{base} and ψ are the transmission parameters to be fitted for the POIs and CBGs, respectively. Chang et al. (2021) defined that the transition from the susceptible group to the exposed group in equation (1) originates from the fact that the transition of individuals belonging to the susceptible group visit POIs with infectious peoples and depends on the transmission within each CBG. The effect of mobility reduction is reflected in $w_{ij}^{(t)}$. Therefore, it is straightforward to evaluate NPIs that reduce the spread of COVID-19 by examining mobility changes.

However, several difficulties arise when the ESEIR model is applied to the COVID-19 situation in Seoul. First, there are many residential-commercial complexes in Seoul, and the density of commercial facilities and shops in each building is very high, making it difficult to determine which facilities a person visits in a building from mobile information. Thus, it is very difficult to apply the concept of CBGs and POIs to a megacity such as Seoul. Second, there has been a ban on gatherings to reduce transmission in Korea, which is quite effective, but the reduction mechanism is considered to differ from that of social distancing, which is discussed below. Because Chang et al. (2021)'s ESEIR model focuses only on mobility changes, it should be modified to reflect the effect of the ban on gatherings, as it affects human behavior in commercial facilities where mass infections may arise.

3.3. A new modified ESEIR model

The previous ESEIR model cannot be directly applied to Seoul. Rather than using concepts such as CBGs and POIs, we consider the administrative geographical unit (gu) and mobility between gu as being reasonable for analysis because dong is too small to guarantee a sufficient number of new confirmed cases. Gu is a second-level administrative unit whose associated population size ranges from 136,030 to 678,067. We believe that modelling gu as a single unit for COVID-19 transmission provides a reasonable approximation for assessing the impact of NPIs in Seoul. Although data at the level of smaller administrative units (i.e., dong) may provide a higher resolution, modelling at the dong level is impractical, as the number of new confirmed cases in each dong is quite limited during the period in which our study refers to and the number of dongs in Seoul was high ($n = 426$). Because CBGs and POIs are no longer relevant concepts in our application, the dwell time fraction d_{p_j} and physical area a_{p_j} are not used. Additionally, considering that the actual mobility reduction after implementating the ban on gatherings is about 4% during the study period, it is not reasonable to introduce a 58% reduction in mobility to explain the observed reduction in the daily number of new confirmed cases during the same period. To explain these observations, the ban on gatherings should be reflected in the mathematical model in a manner different from the method used to reflect the mobility. Unlike social distancing, the ban on gatherings greatly contributes to reducing mass infection risks in restaurants, coffee shops, karaoke, and sports facilities.

Therefore, we modified the ESEIR model as follows.

$$S_i^{(t+1)} = S_i^{(t)} - N_{S_i \to E_i}^{(t)} - v_i^{(t)} \tag{3}$$

$$N_{S_i \to E_i}^{(t)} \sim \underbrace{\text{Poisson}\left(\beta_i K_i^{\alpha} \frac{S_i^{(t)}}{N_i} \sum_{j \neq i} I_j^{(t)} w_{ji}^{(t)}\right)}_{\text{between effect}} + \underbrace{\text{Poisson}\left(\eta_i K_i^{\alpha} \frac{S_i^{(t)}}{N_i} I_i^{(t)} w_{ii}^{(t)}\right)}_{\text{within effect}} \tag{4}$$

where β_i and η_i are the between-and within-transmission parameters, respectively, to be estimated. $w_{ji}^{(t)}$ is the number of people moving from jth gu to ith gu at time t, K_i is the number of commercial facilities in ith gu and $\alpha(\geq 0)$ is the control parameter for the effect of the ban on gatherings. Additionally, $v_i^{(t)}$ denotes the number of fully vaccinated individuals in ith gu at time t.

In the modified equation, the number of individuals moving from S to E is decomposed into two parts. Considering ith gu, the first part describes how incoming mobility from other regions and the unique characteristic related to mass

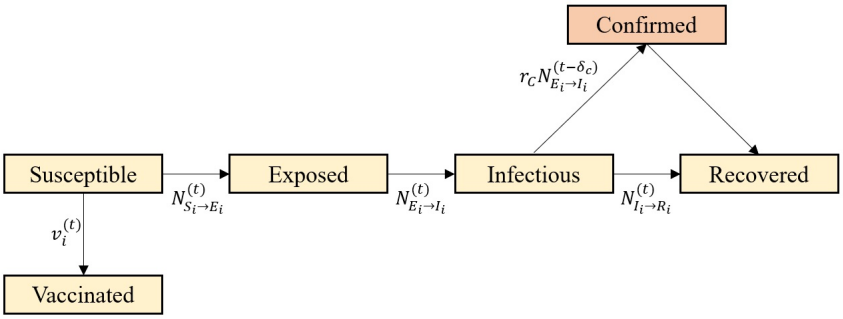

Figure 4: Compartmental structure of the proposed ESEIR model.

Parameter	Description	Value	Reference
β_i	Between transmission parameter	Estimated	-
η_i	Within transmission parameter	Estimated	-
α	Control parameter for the effect of the ban on gatherings	Estimated	-
δ_E	Latent period	3	Zhao et al. (2021)
δ_I	Infectious period	4	Hart et al. (2022)
δ_C	Duration of confirmation after becoming infectious	4	Song et al. (2020)
r_C	Proportion of detected cases among infectious	$0.5^{\dagger}$	Lee et al. (2021)

† The detailed calculation is provided in Supplementary material

Table 1
Description of the model parameters

infection risks in *i*th gu affects transmission. The second part describes how mobility within *i*th gu and its mass infection risk characteristics that affect the transmission. This decomposition was inspired by the between-within effect in the endemic-epidemic modelling framework proposed by Held et al. (2005).

Effects of the ban on gatherings are reflected in $\beta_i K_i^{\alpha}$ and $\eta_i K_i^{\alpha}$, where α can change before and after the ban on gatherings was implemented. The exponentiation forms allow for a nonlinear relationship between the number of commercial facilities K_i and the average number of individuals who transitioned from S to E. Nonlinearity is related to the heterogeneous disease characteristics of the population, which are characterized by probability distributions for susceptibility and infectivity. Dass et al. (2021) explained how the resulting epidemic model that includes heterogeneity leads to the power transmission dynamics. Novozhilov (2012) also showed that the power-law function can be inferred from heterogeneous susceptible, infectious, and recovered models. McCallum et al. (2001) explained this point from a different perspective, stating that non-linearity is necessary to describe a real situation phenomenologically. However, this does not mean that only the exponentiation form is allowed in our application. Other functional forms can be considered. In fact, we compare the predictive performance of the exponentiation form (K_i^{α}) with that of the linear form (αK_i) within our research period. We decide to report the results from the exponentiation function only here because of its better prediction performance (Table S2), and some prediction results from the linear form are provided in Supplementary material (Figure S9). To provide more clues to why the power-law function is appropriate, we also check the relationship between the number of commercial facilities and the amount of mobility, and investigate how much the cut-off change of the ban on gatherings affects the differences of new confirmed cases between before and after the ban on gatherings. These plots are provided in Supplementary material. In addition to the exponentiation form, we included the effect of vaccination by subtracting the number of fully vaccinated individuals from the number of susceptible individuals. We assume that fully vaccinated people with two doses of Pfizer-BioNTech, Moderna, or AstraZeneca vaccine, or a single dose of the Janssen vaccine, are protected from infection.

To estimate the parameters in the proposed ESEIR model, we maximized the Poisson likelihood for the observed number of daily new confirmed cases; its mathematical expression is provided in the Appendix. The 95% prediction

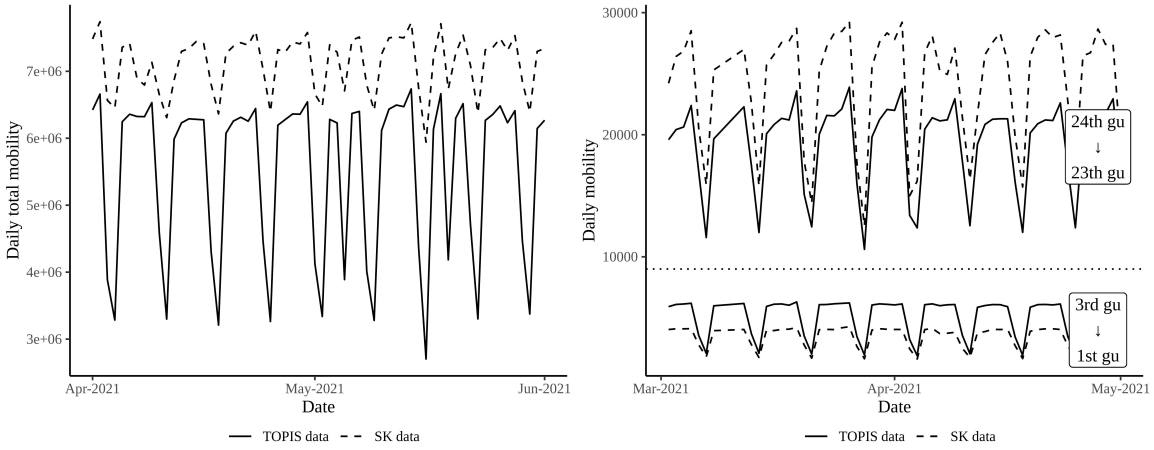

(a) The daily total value

(b) The daily value in specific direction

Figure 5: Mobility pattern between two mobility data types

interval for new confirmed cases was obtained by calculating the 2.5% and 97.5% percentiles of 5,000 prediction values generated from the fitted model. The number of new confirmed cases differed according to the number of infected individuals. To link these two values, we considered the duration and proportion of confirmation among the infected individuals, as in Chang et al. (2021). The expected daily number of new confirmed cases in ith gu at time t, denoted by $\hat{c}_i^{(t)}$, can be expressed as: $\hat{c}_i^{(t)} = r_C N_{E_i \to I_i}^{(t-\delta_C)}$ where r_C is the proportion of confirmed cases among infected individuals and δ_C is the duration of confirmation after becoming infectious. To reflect these points, the compartmental structure of the proposed ESEIR model is shown in Figure 4 and the parameters are listed in Table 1.

3.4. Finding the relationship between the two mobility data

Because the SK mobility data are available from March to July 2021, the research period was limited. Considering that the TOPIS mobility data are available without limitations, we studied the relationship between SK and the TOPIS mobility data. If the two mobility values have an explicit functional relationship, we can estimate the SK mobility data accurately using the TOPIS mobility data.

Figure 5a shows a plot of the aggregate daily mobility values in Seoul based on the TOPIS and SK data. Mobility values from mobile information were greater than those from public transportation. Although their overall patterns were similar, the mobility difference between weekdays and weekends was larger in the TOPIS data. Figure 5b shows the daily mobility values in two directions. The upper and lower parts, which are above and below the dotted horizontal line, represent the daily mobility values from 24th gu to 23rd gu and 3rd gu to 1st gu, respectively. The upper part shows that the SK mobility value is larger than that from TOPIS, whereas the lower part shows the opposite result. A reason for this observation is detailed explained in Supplementary material. As such, the data that will result in a larger value depends on the characteristics of gu, and separate regression models based on gu are necessary to determine the relationship between the two mobility values.

We considered two Poisson regression models, with the weekend indicator variable as covariate. Suppose that $S_{ijt} \sim \text{Poisson}(\mu_{ijt})$ where S_{ijt} is the SK mobility value from ith gu to jth gu at time t and μ_{ijt} denotes the expectation value of S_{ijt}. The two models are expressed as follows:

$$\text{Model 1 } (f^1): \ \log \mu_{ijt} = \beta_0 + \beta_1 P_{ijt} + \beta_2 W_t$$
$$\text{Model 2 } (f_{ij}^2): \ \log \mu_{ijt} = \beta_{ij0} + \beta_{ij1} P_{ijt} + \beta_{ij2} W_t$$

where P_{ijt} is the TOPIS mobility value and $W_t = 1$ when time t corresponds to the weekend and otherwise 0. Model 1 describes the mobility relationship using global regression coefficients. These values are constant across administrative

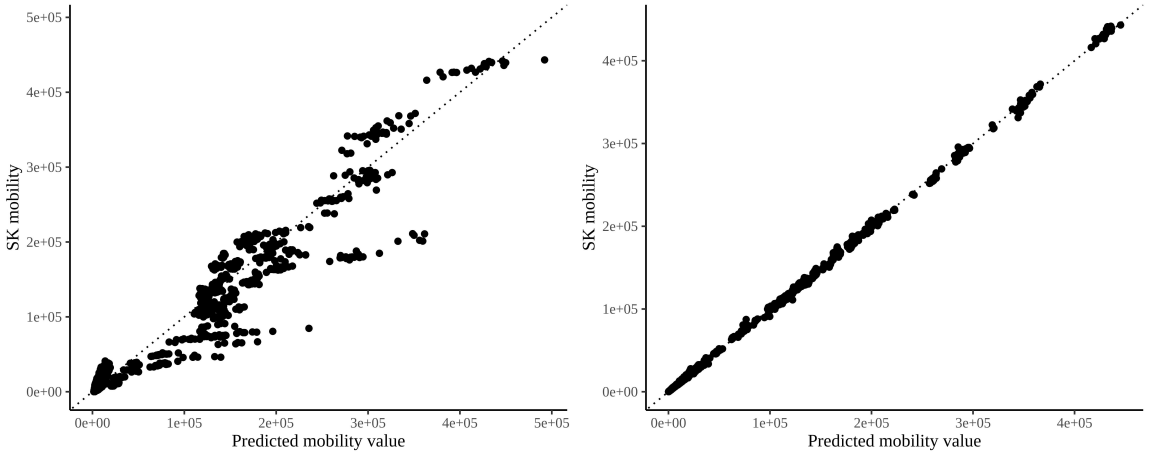

Figure 6: Result of estimating OD matrices.

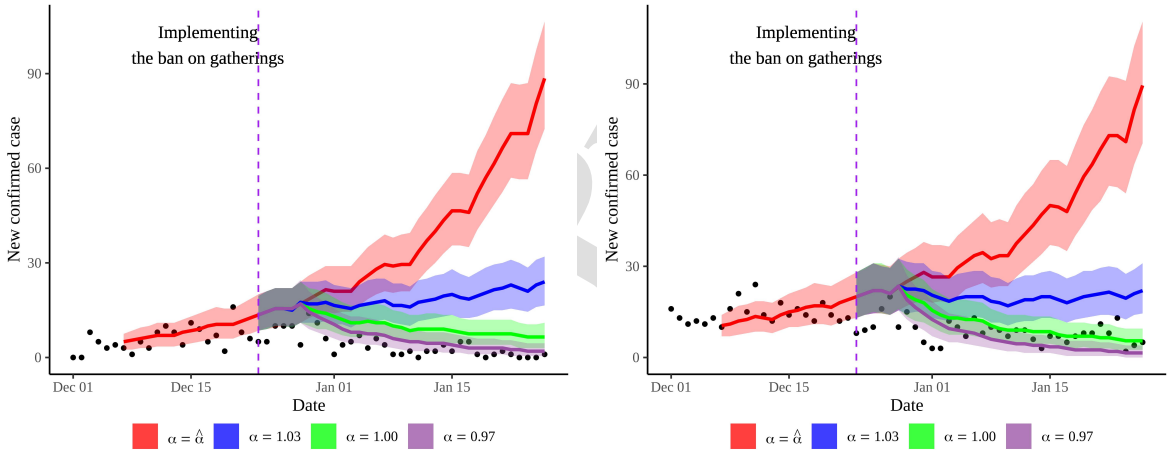

(a) Result in Geumcheon-gu

(b) Result in Gangnam-gu

Figure 7: Prediction result for the effect of the ban on gatherings.

geographical units. In contrast, the regression coefficients of Model 2 are direction-dependent (moving from *i*th to *j*th gu).

The two Poisson models were fitted to the training data from March to May 2021 and the prediction performance was assessed for the test period from June 1 to June 30. In Figure 6, the x- and y-axes represent the predicted and observed mobility values for the test period, respectively. Model 2 showed almost perfect linearity and its predictive R-squared (R^2) and RMSE were 0.999 and 80,100, respectively, which were much better than those of Model 1 with predictive R-squared = 0.950 and RMSE = 1,081,704. Therefore, Model 2 was used to predict the SK OD matrices from November 2020 to November 2021 using TOPIS data.

4. Result

4.1. Effect of NPIs

To control the rapidly increasing number of new confirmed cases in Seoul, level 2.5 social distancing was implemented on December 8, 2020, and the ban on gatherings was additionally implemented on December 23, 2020.

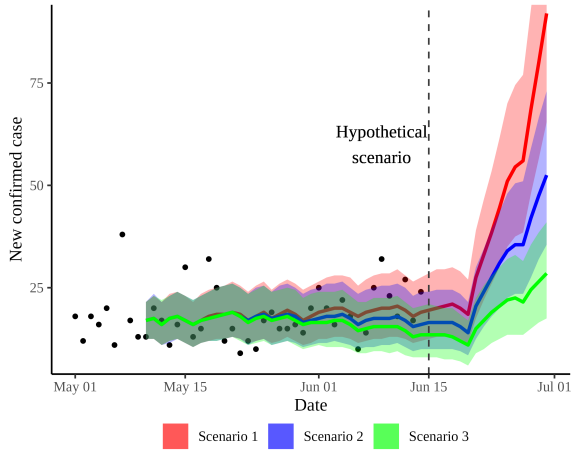

Figure 8: Prediction result for the effect of vaccination in Gangnam-gu

We investigated the effects of social distancing and the ban on gatherings using the proposed ESEIR model based on the observed mobility information. The training period (period used to fit the model) was until December 7, 2020 (the day before level 2.5 social distancing was implemented), and compared the model-based predictions with real data for the next 50 days. Especially, we ask how much the predicted number of confirmed cases changes if the ban on gatherings is implemented on December 23. To answer for this question before implementing the ban on gatherings, we consider hypothetical scenarios with reasonably chosen alpha values. To represent the effect of the ban on gatherings, we considered a set of $\alpha \in \{0.97, 1.00, 1.03, 1.06\}$ where $1.06(= \hat{\alpha})$ is the estimated value of α from the training period. Making predictions with $\hat{\alpha}$ corresponds to the fact that the ban on gatherings can affect the mobility term only in the ESEIR model because $\hat{\alpha}$ is the same as in the training period. As shown in Figure 7, the four colored lines indicate the predicted numbers of new confirmed cases in Geumcheon-gu and Gangnam-gu depending on the different α values, and the corresponding shaded areas are 95% prediction intervals based on the ESEIR model. As α decreased, the predicted numbers also decrease. A discrepancy was observed between the observed and predicted numbers when $\alpha = \hat{\alpha}$ (red line) after the declaration of the ban on gatherings; thus, using the observed mobility reduction alone cannot explain the new confirmed cases for 50 days after the training period (black dots). The effect of the ban on gatherings is well represented using $\alpha = 0.97$, which corresponds to the value with the best prediction performance. See Table S2. If we attempt to explain the actual value only through mobility reduction, which presumes that there is no change in α, the observed mobility must be lowered by 58%, which is not realistic. Therefore, level 2.5 social distancing, with a focus on reducing mobility, and the ban on gatherings, with a focus on reducing mass infection risks, have different effects on the number of new confirmed cases. The Seoul Metropolitan Government reported that the increasing proportion of mass infections changed to a decreasing trend after the implementation of the a ban on gatherings (Bureau of Civil Health, Seoul Metropolitan City Government, 2021).

4.2. Effect of NPIs when vaccination is in progress

Vaccination in Korea began in February 2021, and the ban on gatherings was maintained until May, and the social distancing was lifted to level 2 on February 15. As NPIs negatively affect the financial situation of small businesses, the government is interested in the optimal timing for NPIs to be lifted. In this section, the key question is about whether NPIs can be lifted following vaccine development. First, we ask how much the predicted number of confirmed cases changes if the vaccination number increases. Three hypothetical vaccination scenarios are considered: (1) maintaining the actual number of vaccinations, (2) vaccinations three times more than the number in scenario 1 and (3) vaccinations five times more than the number in scenario 1. Data compiled before May 10 were used to fit the model. We first compared the predicted number of new confirmed cases until June 14 under the three scenarios. Assuming that the ban on gatherings is maintained at the current level, the left of the dashed vertical line in Figure 8 shows the prediction results until June 15, 2021. Even when the number of vaccinations was increased five times, the number of new confirmed cases did not significantly decrease. Therefore, increasing the number of vaccinations

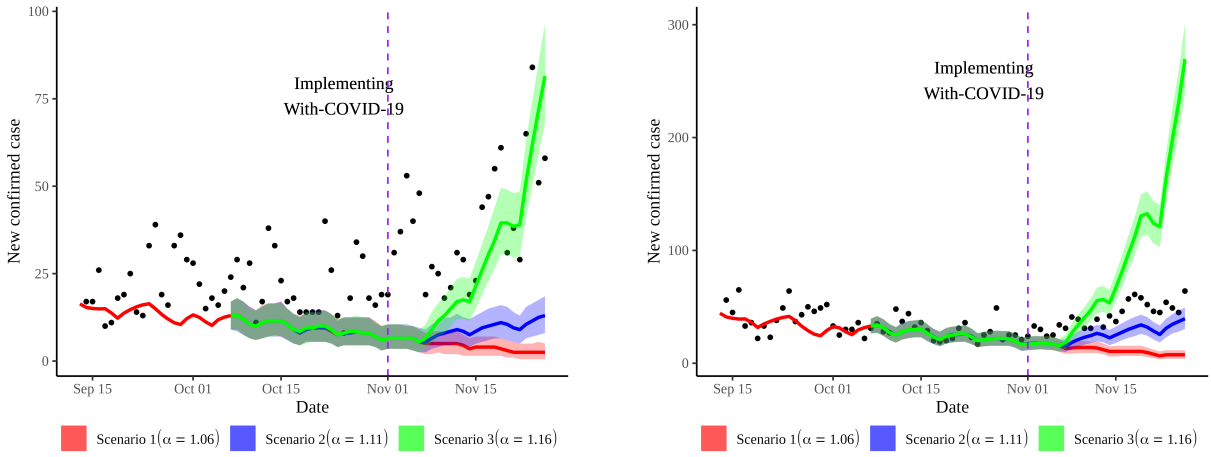

(a) Result in Geumcheon-gu

(b) Result in Gangnam-gu

Figure 9: Prediction result for the effect of With-COVID-19

alone is insufficient to substantially reduce the number of new confirmed cases because the number of vaccinations was relatively small compared with the size of the susceptible group during that period.

Next, we ask how much the predicted number of new confirmed cases changes if the ban on gatherings is lifted from June 15. To answer for this question before lifting the ban on gatherings, we consider hypothetical scenarios with reasonably chosen alpha values. In this application, the lift is represented as the increase in α up to 1.10 from an estimated value of 1.03. The right of the dotted vertical line in Figure 8 shows the prediction results under each vaccination scenarios if the ban on gatherings is lifted on June 15. The numbers of vaccinated and cumulative vaccinations were 57,409 and 627,708, respectively, on June 15. A rapidly increasing infection pattern was observed after the ban on gatherings was lifted, even after vaccinations increased. Therefore, the role of NPIs is important at the beginning of vaccine development. Actually, around Jun 15 and after, our government did not lift the ban on gatherings so that the actual number of new confirmed cases is not be compared to the prediction results from the hypothetical scenarios.

4.3. Effect of declaring a return to normal in Seoul

The Korean government declared a return to normal on November 1, 2021, known as 'With-COVID-19'. After this declaration, the number of people allowed to gather increased from two to ten. Going back before November 1, we ask how much the predicted number of new confirmed cases changes if With-COVID-19 is declared from November 1. To answer for this question before the declaration, we consider hypothetical scenarios with reasonably chosen alpha values. We first fitted the proposed ESEIR model using the data until October 7, and the estimate of α was 1.06. The number of new confirmed cases was predicted from October 8, and the effect of the with-COVID-19 declaration was predicted from November 1 under the following three scenarios: (1) maintaining α at 1.06, (2) the lift changes α up to 1.11 on November 1, and (3) the lift changes α up to 1.16 on November 1.

Figure 9 shows the predicted number of new confirmed cases in November for Geumcheon-gu and Gangnam-gu. Scenario 1 shows large discrepancies between the predicted values and observations. Therefore, to explain the effect of the lift by declaration, it is necessary to consider the changed value of α. In Seoul, the predicted value under scenario 3 ($\alpha = 1.12$) matches well with the actual values in Geumcheon-gu, and the same α is effective for many gu, as shown in Figure 10. However, a single α value does not accurately describe all gu. In Gangnam-gu, Dongdaemun-gu, Guro-gu, Gwangjin-gu, Jongno-gu, Jung-gu, Mapo-gu, Seongdong-gu and Songpa-gu, scenario 2 ($\alpha = 1.07$) appears to better represent reality.

5. Discussion

We modified the existing ESEIR model to study the effects of various NPIs and vaccinations for COVID-19 in Seoul. First, we showed that the modified ESEIR model captured the pattern of the number of confirmed cases in Seoul in response to the change in the ban on gatherings policy, and explained how the effect of social distancing differs from that of the ban on gatherings in Seoul using the model. Second, we studied whether the ban on gatherings was necessary under various vaccination scenarios. Third, we analyzed the effect of declaring a return to normal and how much a lift of the ban on gatherings in Seoul increases the number of new confirmed cases through the proposed ESEIR model. Finally, we overcame the limitation of the available period of SK mobility data by investigating the relationship between them and public TOPIS mobility data.

The ban on gatherings aims to mitigate the high risk of mass infection in various facilities, such as restaurants, coffee shops, megachurches, and large sports facilities. The large differences between the observed and predicted values depend on whether the ban on gatherings is implemented, indicating that mitigating the mass infection risks in commercial facilities plays an important role in government quarantine measures.

Our findings also emphasize the importance of NPIs even after vaccination. During the initial period of vaccination, the number of vaccinations was relatively small compared to the size of the susceptible group. It is essential to maintain social distancing and gathering bans for some time. Our model shows that the number of new confirmed cases can rapidly increase if the ban on gatherings is prematurely lifted.

As the proportion of detected cases among the infected, r_C, has not been investigated in detail, hence the value used in this study, $r_C = 0.5$, can be uncertain. To address this uncertainty, we performed a sensitivity analysis for different values of r_C ($r_C = 0.4$ and $r_C = 0.6$); the results are provided in the supplementary material (Figure S1-S8). Our findings remain consistent under different conditions.

Our study had some limitations. First, the age structure of the population of interest has a large impact on COVID-19 transmission and severity, but this is not reflected in our model. In addition, the different timing of vaccination by age can be a concern to our model if the research period is close to when vaccination began. The age-aggregated SEIR model may not capture the impact of NPIs fully if the timing of vaccination is sufficiently different by age. In our research period, because diverse age groups have been vaccinated, this different timing issue may not be a big concern, but careful interpretation of the model results may be required because the vaccination is not completely uniform across age. Some interesting extensions to age-structure dependent SEIR models are shown in Yang et al. (2021) and Blyuss and Kyrychko (2021). In addition, the proposed ESEIR model assumes that variations in the mobility reflect the transmission dynamics of COVID-19 well. This assumption is plausible if individuals who have had vaccinations and those who have not are uniformly mixed. Otherwise, the goodness-of-fit of the proposed SEIR model may decrease because the increased mobility of socially active groups that are immunized does not always imply the increase of new confirmed cases. Second, the current model assumes that asymptomatic cases are detected as well as symptomatic cases. This may be the case during the period in which our study is concerned (i.e., the number of cases is not too high) and intensive contact tracing was then performed. Additional modifications for the proposed ESEIR model may be needed when it is applied to a period in which the number of cases is high. Third, there is a population movement between Seoul and other areas. The current model assumes a closed population in Seoul. The number of confirmed cases is likely to be affected by population migration into and out of Seoul. In addition, the suggested model might not adequately capture the transmission dynamics of SARS-CoV-2. Considering that Seoul is geographically surrounded by Gyeonggi province, it is necessary to investigate how the cases confirmed in Gyeonggi are involved in the transmission dynamics in Seoul. However, this requires additional data about the population movement between Seoul and Gyeonggi and the cases confirmed in Gyeonggi by a proper administrative unit, which are not currently available. Therefore, this investigation is beyond the scope of the current study. Fourth, our model assumes that there is no reinfection when an infected person has recovered or when a person in the susceptible group is fully vaccinated. However, recent research has shown that a vaccine breakthrough infection can occur even in a fully vaccinated person (CDC COVID-19 Vaccine Breakthrough Case Investigations Team, 2021).

In addition, the SARS-COV-2 virus constantly mutates, creating variants that can affect COVID-19 diagnosis and key epidemiological parameters used in ESEIR models, such as the latent and incubation periods (Jansen et al., 2021). Finally, the parameter representing the effect of the ban on gatherings, α, may be heterogeneous depending on the characteristics of each region. In such cases, additional modelling is required to explain the heterogeneity.

6. CRediT authorship contribution statement

Seungpil Jung: Methodology, Software, Validation, Formal analysis, Data curation, Writing original draft. **Jong-Hoon Kim**: Conceptualization, Methodology, Writing review & editing. **Seung-Sik Hwang**: Writing review & editing. **Junyoung Choi**: Funding acquisition, Writing review & editing. **Woojoo Lee**: Conceptualization, Supervision, Methodology, Investigation, Writing original draft, review & editing.

7. Declaration of competing interest

The authors declare that they have no known competing interests or personal relationships that could have appeared to influence the work reported in this paper.

8. Acknowledgement

This study was exempted from review by the Institutional Review Board (IRB) of Seoul National University (SNUIRB-2022-NH-001) because the data were aggregated and anonymized. Woojoo Lee was supported by the National Research Foundation of Korea (NRF) grant funded by the Korea government (MSIT) (no. 2021R1A2C1014409). This work was supported by the National Research Foundation of Korea (BK21 Center for Integrative Response to Health Disasters, Graduate School of Public Health, Seoul National University). This research was funded by the Seoul Institute of Technology (SIT) (2020-MR-004, Development of Smart City Epidemic Simulation Model using the Mobile Telecommunication Big Data based Spatio-Temporal Simulation).

9. Appendix

To implement the proposed ESEIR model, a set of initial values for each compartments (S, E, I, and R) is required. We modified Kondo (2021)'s approach to construct the initial values for each compartment, as follows:

$$R_i^{(t)} = \frac{1}{r_C} C_i^{(t+\delta_C-\delta_I)}, \qquad I_i^{(t)} = \frac{1}{r_C} C_i^{(t+\delta_C)} - R_i^{(t)}$$
$$E_i^{(t)} = \frac{1}{r_C} C_i^{(t+\delta_C+\delta_E)} - \frac{1}{r_C} C_i^{(t+\delta_C)}, \qquad S_i^{(t)} = N_i^{(t)} - E_i^{(t)} - I_i^{(t)} - R_i^{(t)}$$

where $C_i^{(t)}$ is the cumulative confirmed cases at time t in ith gu; δ_E and δ_I are the latent and infectious periods, respectively; δ_C is the duration of confirmation after becoming infectious, and r_C is the proportion of confirmation among infectious.

To fit the proposed ESEIR model. we used `optim()` in R. To guarantee the positivity of the transmission parameters, we used the following parameterizations $\beta_i = e^{\beta_i^*}$, $\eta_i = e^{\eta_i^*}$ and $\alpha = e^{\alpha^*}$, which allows β_i^*, η_i^* and α^* to move from $-\infty$ to ∞. The parameter estimates are obtained by maximizing the log Poisson likelihood function, written as

$$l(\beta, \eta, \alpha) = \sum_{i=1}^{25} \sum_{t=1}^{n} \left[c_i^{(t)} \log \left\{ \mathbb{E}\left(\hat{c}_i^{(t)}\right) \right\} - \mathbb{E}\left(\hat{c}_i^{(t)}\right) \right]$$

where $c_i^{(t)}$ and $\hat{c}_i^{(t)}$ are the observed and estimated daily numbers of new confirmed cases in ith gu at time t, respectively, and $\beta = (\beta_1, ..., \beta_{25})$ and $\eta = (\eta_1, ..., \eta_{25})$ are the between and within transmission parameter vectors (25 gu in Seoul). We use $\hat{c}_i^{(t)} = r_C N_{E_i \to I_i}^{(t-\delta_C)}$ given in Section 3.3,

$$\mathbb{E}\left(\hat{c}_i^{(t)}\right) = \mathbb{E}\left(r_C N_{E_i \to I_i}^{(t-\delta_C)}\right) = \frac{r_C}{\delta_E} E_i^{(t-\delta_C)}$$

where $E_i^{(t-\delta_C)}$ is the number of individuals belonging to E in ith gu at time $t - \delta_C$, and $E_i^{(t-\delta_C)}$ is calculated as

$$E_i^{(t-\delta_C)} \approx E_i^{(t-\delta_C-1)} + \mathbb{E}\left(N_{S_i \to E_i}^{(t-\delta_C-1)}\right) - \mathbb{E}\left(N_{E_i \to I_i}^{(t-\delta_C-1)}\right)$$

$$
\begin{aligned}
&= E_i^{(t-\delta_C-1)} + \mathbb{E}\left(N_{S_i\to E_i}^{(t-\delta_C-1)}\right) - \frac{1}{\delta_E}E_i^{(t-\delta_C-1)} \\
&= E_i^{(t-\delta_C-1)}\left(1-\frac{1}{\delta_E}\right) + \mathbb{E}\left(N_{S_i\to E_i}^{(t-1)}\right) \\
&= E_i^{(0)}\left(1-\frac{1}{\delta_E}\right)^{t-\delta_C} + \sum_{k=1}^{t-\delta_C}\mathbb{E}\left(N_{S_i\to E_i}^{(t-\delta_C-k)}\right)\left(1-\frac{1}{\delta_E}\right)^{k-1}
\end{aligned}
$$

where $E_i^{(0)}$ is the initial value of $E_i^{(t)}$, and

$$
\mathbb{E}\left(N_{S_i\to E_i}^{(t-\delta_C-k)}\right) = \beta_i K_i^{\alpha}\frac{S_i^{(t-\delta_C-k)}}{N_i}\sum_{j\neq i} I_j^{(t-\delta_C-k)} w_{ji}^{(t-\delta_C-k)} + \eta_i K_i^{\alpha}\frac{S_i^{(t-\delta_C-k)}}{N_i} I_i^{(t-\delta_C-k)} w_{ii}^{(t-\delta_C-k)}
$$

.

References

Abbey, H. 1952. An examination of the Reed-Frost theory of epidemics. Hum Biol, 24(3), 201-233. https://www.ncbi.nlm.nih.gov/pubmed/12990130

Andersson, H. & Britton, T. 2000. Stochastic Epidemic Models and Their Statistical Analysis. Volume 151. Springer, New York. https://doi.org/10.1007/978-1-4612-1158-7

Badr, H. S., Du, H. R., Marshall, M., Dong, E. S., Squire, M. M., & Gardner, L. M. 2020. Association between mobility patterns and COVID-19 transmission in the USA: a mathematical modelling study. Lancet Infectious Diseases, 20(11), 1247-1254. https://doi.org/10.1016/S1473-3099(20)30553-3

Becker, N. 1981. A general chain binomial model for infectious diseases. Biometrics, 37(2), 251-258. https://www.ncbi.nlm.nih.gov/pubmed/7272413

Blyuss, K. B., & Kyrychko, Y. N. 2021. Effects of latency and age structure on the dynamics and containment of COVID-19. J Theor Biol, 513, 110587. https://doi.org/10.1016/j.jtbi.2021.110587

Britton, T., Ball, F., & Trapman, P. 2020. A mathematical model reveals the influence of population heterogeneity on herd immunity to SARS-CoV-2. Science, 369(6505), 846-849. https://doi.org/10.1126/science.abc6810

Bureau of Civil Health, Seoul Metropolitan City Government. 2021. The daily news review. Seoul Metropolitan Government. https://www.seoul.go.kr/coronaV/coronaStatus.do?menu_code=07 (accessed 19 May 2022)

Chang, S., Pierson, E., Koh, P. W., Gerardin, J., Redbird, B., Grusky, D., & Leskovec, J. 2021. Mobility network models of COVID-19 explain inequities and inform reopening. Nature, 589(7840), 82-87. https://doi.org/10.1038/s41586-020-2923-3

Choi, S., & Ki, M. 2020. Estimating the reproductive number and the outbreak size of COVID-19 in Korea. Epidemiol Health, 42, e2020011. https://doi.org/10.4178/epih.e2020011

Dass, S. C., Kwok, W. M., Gibson, G. J., Gill, B. S., Sundram, B. M., & Singh, S. 2021. A data driven change-point epidemic model for assessing the impact of large gathering and subsequent movement control order on COVID-19 spread in Malaysia. PLoS One, 16(5), e0252136. https://doi.org/10.1371/journal.pone.0252136

Food and Drug Administration. 2022. COVID-19 Vaccines. Coronavirus Disease 2019 (COVID-19). https://www.fda.gov/emergency-preparedness-and-response/coronavirus-disease-2019-covid-19/covid-19-vaccines (accessed 19 May 2022)

Hart, W. S., Miller, E., Andrews, N. J., Waight, P., Maini, P. K., Funk, S., & Thompson, R. N. 2022. Generation time of the alpha and delta SARS-CoV-2 variants: an epidemiological analysis. Lancet Infect Dis, 22(5), 603-610. https://doi.org/10.1016/S1473-3099(22)00001-9

Held, L., Höhle, M., & Hofmann, M. 2005. A statistical framework for the analysis of multivariate infectious disease surveillance counts. Statistical Modelling, 5(3), 187-199. https://doi.org/10.1191/1471082X05st098oa

Jansen, L., Tegomoh, B., Lange, K., Showalter, K., Figliomeni, J., Abdalhamid, B., Iwen, P. C., Fauver, J., Buss, B., & Donahue, M. 2021. Investigation of a SARS-CoV-2 B.1.1.529 (Omicron) Variant Cluster - Nebraska, November-December 2021. MMWR Morb Mortal Wkly Rep, 70(5152), 1782-1784. https://doi.org/10.15585/mmwr.mm705152e3

Kim, S. K. 2007. The estimation and application of origin-destination tables by using smart card data, Research Report, Seoul Development Institute, Korea. https://www.si.re.kr/node/24320

Kondo, K. 2021. Simulating the impacts of interregional mobility restriction on the spatial spread of COVID-19 in Japan. Scientific Reports, 11(1). https://doi.org/10.1038/s41598-021-97170-1

Lee, C., Apio, C., & Park, T. 2021. Estimation of Undetected Asymptomatic COVID-19 Cases in South Korea Using a Probabilistic Model. Int J Environ Res Public Health, 18(9). https://doi.org/10.3390/ijerph18094946

Lekone, P. E., & Finkenstadt, B. F. 2006. Statistical inference in a stochastic epidemic SEIR model with control intervention: Ebola as a case study. Biometrics, 62(4), 1170-1177. https://doi.org/10.1111/j.1541-0420.2006.00609.x

Lim, C., Nam, Y., Oh, W. S., Ham, S., Kim, E., Kim, M., Kim, S., Kim, Y., & Jeong, S. 2022. Characteristics of transmission routes of COVID-19 cluster infections in Gangwon Province, Korea. Epidemiol Infect, 150, e19. https://doi.org/10.1017/S0950268821002788

Lopez Bernal, J., Andrews, N., Gower, C., Gallagher, E., Simmons, R., Thelwall, S., Stowe, J., Tessier, E., Groves, N., Dabrera, G., Myers, R., Campbell, C. N. J., Amirthalingam, G., Edmunds, M., Zambon, M., Brown, K. E., Hopkins, S., Chand, M., & Ramsay, M. 2021. Effectiveness

of Covid-19 Vaccines against the B.1.617.2 (Delta) Variant. N Engl J Med, 385(7), 585-594. https://doi.org/10.1056/NEJMoa2108891

McCallum, H., Barlow, N., & Hone, J. 2001. How should pathogen transmission be modelled? Trends in Ecology & Evolution, 16(6), 295-300. https://doi.org/10.1016/S0169-5347(01)02144-9

Medeiros-Sousa, A. R., Laporta, G. Z., Coutinho, R. M., Mucci, L. F., & Marrelli, M. T. 2021. A mathematical model for zoonotic transmission of malaria in the Atlantic Forest: Exploring the effects of variations in vector abundance and acrodendrophily. PLoS Negl Trop Dis, 15(2), e0008736. https://doi.org/10.1371/journal.pntd.0008736

Ministry of Health and Welfare. 2020. Coronavirus Disease-19, Republic of Korea. Regular Briefing of Central Disaster and Safety Countermeasure Headquarters on COVID-19. https://www.mohw.go.kr/eng/nw/nw0101vw.jsp?PAR_MENU_ID=1007&MENU_ID=100701&page=1&CONT_SEQ=354431&SEARCHKEY=TITLE&SEARCHVALUE=regular%20briefing (accessed 19 May 2022)

Ministry of Health and Welfare. 2020. Patient Treatment & Management. http://ncov.mohw.go.kr/en/baroView.do?brdId=11&brdGubun=112&dataGubun=&ncv&contSeq=&board_id= (accessed 19 May 2022)

Ministry of Health and Welfare. 2022. Coronavirus Disease-19, Republic of Korea. http://ncov.mohw.go.kr/en (accessed 19 May 2022)

Nouvellet, P., Bhatia, S., Cori, A., Ainslie, K. E. C., Baguelin, M., Bhatt, S., Boonyasiri, A., Brazeau, N. F., Cattarino, L., Cooper, L. V., Coupland, H., Cucunuba, Z. M., Cuomo-Dannenburg, G., Dighe, A., Djaafara, B. A., Dorigatti, I., Eales, O. D., van Elsland, S. L., Nascimento, F. F.,... Donnelly, C. A. 2021. Reduction in mobility and COVID-19 transmission. Nat Commun, 12(1), 1090. https://doi.org/10.1038/s41467-021-21358-2

Novozhilov, A. S. 2012. Epidemiological Models With Parametric Heterogeneity: Deterministic Theory for Closed Populations. Mathematical Modelling of Natural Phenomena, 7(3), 147-167. https://doi.org/10.1051/mmnp/20127310

Oliver, N., Lepri, B., Sterly, H., Lambiotte, R., Deletaille, S., De Nadai, M., Letouze, E., Salah, A. A., Benjamins, R., Cattuto, C., Colizza, V., de Cordes, N., Fraiberger, S. P., Koebe, T., Lehmann, S., Murillo, J., Pentland, A., Pham, P. N., Pivetta, F.,... Vinck, P. 2020. Mobile phone data for informing public health actions across the COVID-19 pandemic life cycle. Sci Adv, 6(23), eabc0764. https://doi.org/10.1126/sciadv.abc0764

SafeGraph. 2020. Places Schema. https://docs.safegraph.com/docs/places-schema (accessed 19 May 2022)

Song, J. Y., Yun, J. G., Noh, J. Y., Cheong, H. J., & Kim, W. J. 2020. Covid-19 in South Korea - Challenges of Subclinical Manifestations. N Engl J Med, 382(19), 1858-1859. https://doi.org/10.1056/NEJMc2001801

Team, C. C.-V. B. C. I. 2021. COVID-19 Vaccine Breakthrough Infections Reported to CDC - United States, January 1-April 30, 2021. MMWR Morb Mortal Wkly Rep, 70(21), 792-793. https://doi.org/10.15585/mmwr.mm7021e3

Wu, J. T., Leung, K., & Leung, G. M. 2020. Nowcasting and forecasting the potential domestic and international spread of the 2019-nCoV outbreak originating in Wuhan, China: a modelling study. Lancet, 395(10225), 689-697. https://doi.org/10.1016/S0140-6736(20)30260-9

Xie, G. 2020. A novel Monte Carlo simulation procedure for modelling COVID-19 spread over time. Sci Rep, 10(1), 13120. https://doi.org/10.1038/s41598-020-70091-1

Yang, W., Shaff, J., & Shaman, J. 2021. Effectiveness of non-pharmaceutical interventions to contain COVID-19: a case study of the 2020 spring pandemic wave in New York City. J R Soc Interface, 18(175), 20200822. https://doi.org/10.1098/rsif.2020.0822

World Health Organization. 2021. COVID-19 weekly epidemiological update, edition 68, 30 November 2021. World Health Organization. https://apps.who.int/iris/handle/10665/350006 (accessed 19 May 2022)

Zhao, S., Tang, B., Musa, S. S., Ma, S., Zhang, J., Zeng, M., Yun, Q., Guo, W., Zheng, Y., Yang, Z., Peng, Z., Chong, M. K., Javanbakht, M., He, D., & Wang, M. H. 2021. Estimating the generation interval and inferring the latent period of COVID-19 from the contact tracing data. Epidemics, 36, 100482. https://doi.org/10.1016/j.epidem.2021.100482

Zhou, F., Yu, T., Du, R., Fan, G., Liu, Y., Liu, Z., Xiang, J., Wang, Y., Song, B., Gu, X., Guan, L., Wei, Y., Li, H., Wu, X., Xu, J., Tu, S., Zhang, Y., Chen, H., & Cao, B. 2020. Clinical course and risk factors for mortality of adult inpatients with COVID-19 in Wuhan, China: a retrospective cohort study. Lancet, 395(10229), 1054-1062. https://doi.org/10.1016/S0140-6736(20)30566-3

Zhou, Y., Xu, R., Hu, D., Yue, Y., Li, Q., & Xia, J. 2020. Effects of human mobility restrictions on the spread of COVID-19 in Shenzhen, China: a modelling study using mobile phone data. Lancet Digit Health, 2(8), e417-e424. https://doi.org/10.1016/S2589-7500(20)30165-5

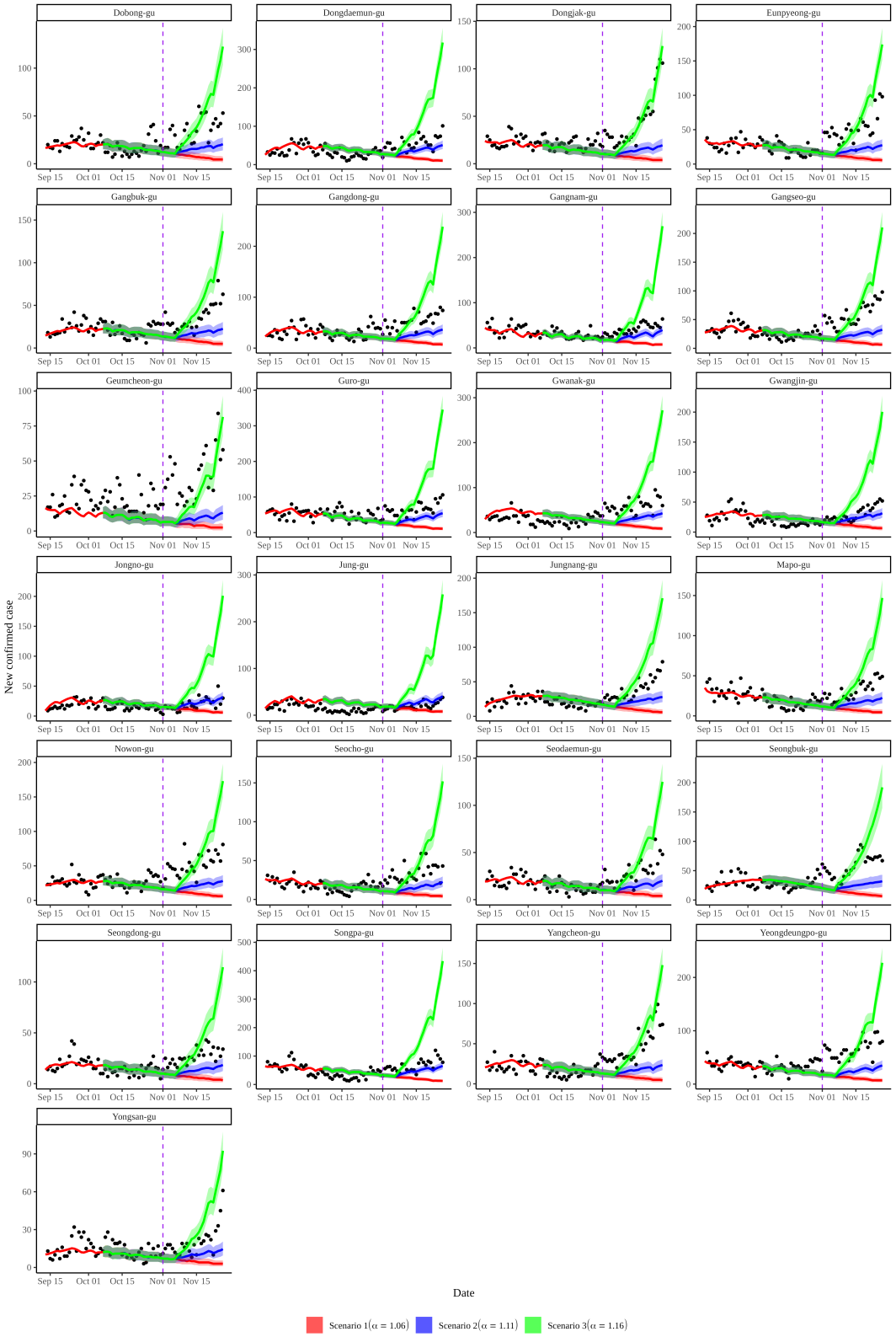

Figure 10: Prediction in With-COVID-19

Highlights

- Seoul has two representative quarantine policies such as social distancing and the ban on gatherings.
- Unlike social distancing, the ban on gatherings aims to mitigate the high risk of mass infection in various facilities
- Effects of these two policies need to be reflected in different functional form in SEIR model.
- A modified SEIR model is proposed to assess the effectiveness of social distancing, ban on gatherings and vaccination strategies.

CRediT authorship contribution statement

Seungpil Jung: Methodology, Software, Validation, Formal analysis, Data curation, Writing – original draft.

Jong-Hoon Kim: Conceptualization, Methodology, Writing – review & editing.

Seung-Sik Hwang: Writing – review & editing.

Junyoung Choi: Funding acquisition, Writing – review & editing.

Woojoo Lee: Conceptualization, Supervision, Methodology, Investigation, Writing – original draft, review & editing.

June 16, 2022

Prof. Dr. Denise Kirschner, Professor Mark Chaplain and Dr. Sasaki
Editors-in-Chief
Journal of Theoretical Biology

Dear Editor:

The authors have no conflicts of interest associated with the material presented in this paper.

Sincerely,
Woojoo Lee PhD
Department of Public Health Science, Graduate School of Public Health, Seoul National University, 1, Gwanak-ro, Gwanak-gu, Seoul, 08826, Republic of Korea
Tel: +82-2-880-2899
E-mail: lwj221@snu.ac.kr